

# Cusps in CDM halos

Jurg Diem<sup>1,3?</sup>, Marcel Zemp<sup>1,2</sup>, Ben Moore<sup>1</sup>, Joachim Stadel<sup>1</sup> & Marcella Carollo<sup>2</sup>

<sup>1</sup> Institute for Theoretical Physics, University of Zurich, Winterthurerstrasse 190, CH-8057 Zurich, Switzerland

<sup>2</sup> Institute of Astronomy, ETH Zurich, ETH Hönggerberg HPP D 6, CH-8093 Zurich, Switzerland

<sup>3</sup> Department of Astronomy and Astrophysics, University of California, 1156 High Street, Santa Cruz CA 95064, USA

11 October 2019

## ABSTRACT

We resolve the inner region of a massive cluster forming in a cosmological CDM simulation with a mass resolution of  $2 \times 10^6 M_\odot$  and before  $z=4.4$  even  $3 \times 10^5 M_\odot$ . This is a billion times less than the cluster's virial mass and a substantial increase over current CDM simulations. We achieve this resolution using a new multiresolution procedure and are now able to probe a dark matter halo density profile down to 0.1 percent of the virial radius. The inner density profile of this cluster halo is well fitted by a power-law  $\rho \propto r^{-n}$  down to the smallest resolved scale. An inner region with roughly constant logarithmic slope is now resolved, which suggests that cuspy profiles describe the inner profile better than recently proposed profiles with a core. The cluster studied here is one out of a sample of six high resolution cluster simulations of Diem and et al. (2004b) and its inner slope of about  $n = 1.2$  lies close to the sample average.

**Key words:** methods: N-body simulations | methods: numerical | dark matter | galaxies: haloes | galaxies: clusters: general

## 1 INTRODUCTION

Recently a great deal of effort has gone into high resolution simulations which have revealed density profiles of cold dark matter halos down to scales well below one percent of the virial radius (Fukushige, Kawai & Makino 2004; Tasitsiomi et al. 2004; Navarro et al. 2004; Reed et al. 2005; Diem and, Moore & Stadel 2004b, "DM S04" hereafter). But the form of profile below 0.5 percent of the virial radius remained unclear and there was no clear evidence for a cusp in the center, i.e. no significant inner region with a constant logarithmic slope. Galaxy cluster halos would be the ideal systems to resolve cusps numerically because of their low concentration. In a galaxy or dwarf halo the inner power law is much harder to resolve because it lies at a smaller radius relative to the size of the system.

The existence of a core or a cusp in the center of CDM halos has important observational consequences and is the crucial point in many tests of the CDM theory. Comparisons of dark matter simulations to rotation curves of low surface brightness galaxies (LSB) seem to favor constant density cores for most observed systems (e.g. Moore 2004; Flores & Primack 1994; Salucci & Burkert 2000; deBlok et al. 2001; see, however van den Bosch & Swaters 2001; Swaters et al. 2003; Simon et al. 2005). But these comparisons still depend to some extent on extrapolations

of the simulated profiles toward the center: Stoehr (2004) extrapolate to a constant density core and claim that the discrepancy to LSB galaxy rotation curves is much smaller than previously believed.

The strength of the  $\gamma$ -ray signal from dark matter annihilation depends on the square of the dark matter density and the calculated flux values spread over several orders of magnitude, depending on how one extrapolates the density profiles from the known, resolved regions down into the centers of the galactic halo and its subhalos (Calcareo-Roldan & Moore 2000; Stoehr et al. 2002; Bertone & Merritt 2005; Prada et al. 2004). Small, very abundant, Earth to Solar mass subhalos could be very luminous in  $\gamma$ -rays if they are cuspy (Diem and et al. 2005).

The highest resolutions in cosmological simulations are reached with the widely used refinement procedure (e.g. Bertschinger 2001): First one runs a simulation at uniform, low resolution and selects halos for re-simulation. Then one generates a new set of initial conditions using the same large scale fluctuations and higher resolution and additional small scale fluctuations in the selected region. With this technique Navarro, Frenk & White (1996) were able to resolve many halos with a few ten thousand particles and to infer their average density profile which asymptotes to an  $\rho(r) \propto r^{-1}$  cusp. Other authors used fitting functions with steeper ( $-1.5$ ) cusps (Fukushige & Makino 1997; Moore et al. 1998; Moore et al. 1999; Ghigna et al. 2000). Small mass CDM halos have higher concentra-

? diem@physik.unizh.ch

tions due to their earlier collapse (Navarro et al. 1996) but the slopes of the inner density profiles are independent of halo mass (Moore et al. 2001; Colin et al. 2004). Open, "standard" and lambda CDM cosmologies, i.e. models with  $(\Omega_m, \Omega_b) = (0.3; 0.0)$ ,  $(1.0; 0.0)$  and  $(0.3; 0.7)$  yield equal inner profiles (Fukushige & Makino 2003; Fukushige, Kawai & Makino 2004). There is some indication that models with less small scale power like WDM lead to shallower inner profiles (e.g. Colin et al. 2000; Reed et al. 2005). Different equation of states of the dark energy component lead to different collapse times and halo concentrations but it is not clear yet if it also affects slopes well inside of the scale radius (Maccio et al. 2004; Kuhlen et al. 2004). Most current simulations do not resolve a large enough radial range to determine both the concentration and the inner slope; at the current resolution these parameters show some degeneracy (Klypin et al. 2001).

Recently a large sample of CDM halos resolved with a million and more particles was simulated (Springel et al. 2001b; Tasitsiomi et al. 2004; Navarro et al. 2004; Reed et al. 2005; Gao et al. 2005) and the best resolved systems contain up to 25 million particles (Fukushige, Kawai & Makino 2004; DM S04). But even these very large, computationally expensive simulations resolved no inner region with a constant logarithmic slope. (Navarro et al. 2004; Stoehr et al. 2002; Stoehr 2004) introduced cored profiles which seem to fit the simulation data better than the cuspy profiles proposed earlier by Navarro et al. (1996) and Moore et al. (1999). This better fit was interpreted as indication against cuspy inner profiles. However these cored profiles have one additional parameter and therefore it is not surprising that they fit the data better. DM S04 showed that an NFW-like profile with the inner slope as additional free parameter fits the highest resolution profiles just as well as cored profiles. Some theoretical arguments seem to favor cusps (e.g. Binney 2004; Hansen & Moore 2004) but make only vague predictions about the inner slopes. A recent model combines simulation results and analytical arguments to predict an inner slope of -1.27 (Ahn & Shapiro 2005). At the moment higher resolution simulations seem to be the only way to decide the core vs. cusp controversy.

Here we present simulations of one of the galaxy clusters from DM S04 with two orders of magnitude better mass resolution. Our results give strong support to cuspy inner profiles. This increase in resolution was made possible with only a moderate increase in computational cost by using a new multi-mass refinement technique described in Section 2. In Section 3 we present our results and in Section 4 the conclusions.

## 2 NUMERICAL EXPERIMENTS

Table 1 gives an overview of the simulations we present in this paper. All runs discussed in this paper model the same CDM cluster labeled "D" in DM S04. With a mass resolution corresponding to  $1.3 \times 10^8$  and  $1.04 \times 10^9$  particles inside the virial radius of a cluster, DM 25 and DM 50 are the highest resolution CDM simulation performed so far. Due to the large number of particles and the corresponding high force and time resolution these runs take a large

amount of CPU time. Fortunately the inner profiles of CDM clusters are already in place around redshift one and evolve little between  $z = 4$  and  $z = 0$  (Fukushige et al. 2004; Tasitsiomi et al. 2004; Reed et al. 2005). Therefore one does not have to run the simulations to  $z = 0$  to gain insight into the inner density profile. We stop DM 50 at  $z = 4.4$ , DM 25 at  $z = 0.8$  and use the medium resolution runs D 5 and D 12 to quantify the low redshift evolution of the density profile of the same cluster. Run DM 25 was completed in about  $2 \times 10^5$  CPU hours on the zBox supercomputer<sup>1</sup>. The convergence radius of run DM 50 is 1.7 kpc, estimated using the  $r/N^{1/3}$  scaling and the measured converged scales from DM S04.

### 2.1 Multi-mass refinements

Often in cosmological N-body simulations one uses high resolution particles only where one halo forms and heavier particles in the surroundings to account for the external tidal forces. One usually tries to define a large enough high resolution region to minimize or avoid mixing of different mass particles within the region of interest. One exception is Binney & Knebe (2002) who used particles of two different masses everywhere to estimate the amount of two body relaxation in cosmological simulations. In plasma simulations on the other hand multi-mass simulations have been successfully used since the 1970s (e.g. Dawson 1983 and refs. therein). Here we apply this idea to increase the resolution in the core of one cluster halo in a cosmological N-body simulation.

The refinement procedure is usually applied to entire virialised systems, i.e. one marks all particles inside the virial radius of the selected halo and traces them back to the initial conditions. Then one refines the region that encloses the positions of the marked particles. Usually the region is further increased to prevent any mixing of low resolution particles into the virial radius of the final system. In DM S04 all particles within 4 comoving Mpc in the initial conditions were added to the high resolution region. This assures that only light particles end up within the virial radius of the final cluster and it also has the advantage that halos in the outskirts of the cluster (out to 2 or 3 virial radii) are still well resolved (Moore et al. 2004). But with this procedure only between one fourth to one third of all the high resolution particles end up in the cluster.

If one is only interested in the inner regions of a halo it is possible to use a new, more efficient way of refinement: Instead of refining the whole virialised system we only refine the region where the inner particles come from. This allows to reduce the size of the high resolution region considerably, because most of particles that end up near the center of the system start in a very small region, compared to the region which one finds by tracing back all the particles inside the virial radius. Using this technique it is possible to reduce the computational cost of a CDM cluster simulation by at least one order of magnitude at equal force and mass resolution in the inner region. Of course now one has different mass particles inside the final virialised structure therefore we must verify that significant equipartition and relaxation

<sup>1</sup> <http://www-theorie.physik.unizh.ch/~stadel/zBox/>

Table 1. Parameters of the simulated cluster. At  $z=0$  the virial mass is  $3:1 \cdot 10^{14} M_{\odot}$  and the virial radius is  $1.75 \text{ Mpc}$ .  $N_{\text{HR}}$  is the number of high resolution particles and  $m_{\text{HR}}$  is the mass and  $r_{\text{HR}}$  the force softening length of these particles. For the multi-mass runs we also give the masses ( $m_{\text{LR}}$ ) and softenings ( $r_{\text{LR}}$ ) of the next heavier particle species. Softening lengths are given at  $z=0$ , "[c]" indicates that a constant softening in comoving coordinates was used, "[p]" indicates that the softening was constant in physical units after  $z=9$  and constant at ten times this value in comoving units before  $z=9$ . The resolved scales are constant in physical units and give the innermost radius we expect to resolve with the given mass resolution.  $N_{\text{vir,e}}$  is the actual number of particles within the virial radius at  $z=0$  for runs D 6, D 9 and D 12. For the multi-mass runs it is the number needed to reach the same resolution in the inner part by doing a conventional refinement of the entire system. All runs are 300 Mpc cubes with periodic boundaries, well outside of the cluster forming region the resolution is decreased (as in DM S04).

Run	$z_{\text{start}}$	$z_{\text{end}}$	$r_{\text{HR}}$ [kpc]	$N_{\text{HR}}$	$m_{\text{HR}}$ [ $M_{\odot}$ ]	$r_{\text{HR}}$ [kpc]	$m_{\text{LR}}$ [ $M_{\odot}$ ]	$r_{\text{resolved}}$ [kpc]	time-step	$N_{\text{vir,e}}$
D 5	52.4	0	4.2[p]	4'898'500	$3:0 \cdot 10^8$	—	—	16.2	0.25	(1) $1:0 \cdot 10^6$
D 6	36.13	0	3.6[p]	31'922'181	$1:8 \cdot 10^8$	—	—	13.5	0.2	(1) $1:8 \cdot 10^6$
DM 6se	36.13	0	3.6[p]	922'968	$1:8 \cdot 10^8$	3.6[p]	$3:8 \cdot 10^{10}$	13.5	0.2	(1) $1:8 \cdot 10^6$
DM 6le	36.13	0	3.6[p]	922'968	$1:8 \cdot 10^8$	38.6[p]	$3:8 \cdot 10^{10}$	13.5	0.2	(1) $1:8 \cdot 10^6$
D 9	40.27	0	2.4[p]	31'922'181	$5:2 \cdot 10^7$	—	—	9.0	0.2	(1) $6:0 \cdot 10^6$
DM 9	40.27	0	2.4[p]	3'115'017	$5:2 \cdot 10^7$	15[p]	$1:4 \cdot 10^9$	9.0	0.2	(1) $6:0 \cdot 10^6$
D 12	43.31	0	1.8[p]	14'066'458	$2:2 \cdot 10^7$	—	—	6.8	0.2	(1) $1:4 \cdot 10^7$
DM 25	52.4	0.8	0.84[c]	65'984'375	$2:4 \cdot 10^6$	9[c]	$3:0 \cdot 10^8$	3.3	0.25	(2) $1:3 \cdot 10^8$
DM 25lt	52.4	0.8	0.84[p]	65'984'375	$2:4 \cdot 10^6$	9[p]	$3:0 \cdot 10^8$	3.3	0.25	(1) $1:3 \cdot 10^8$
DM 50	59.3	4.4	0.36[c]	16'125'000	$3:0 \cdot 10^5$	6[c]	$3:75 \cdot 10^7$	1.7	0.25	(2) $1:0 \cdot 10^9$

(Binney & Knebe 2002; Diemand et al. 2004a) is not occurring and affecting the final results. In section 2.3 we show that the density profiles of such multi-mass clusters (runs DM 6le and DM 9) are the same as the ones of fully refined clusters at equal peak resolution (runs D 6 and D 9).

In this paper we apply the multi-mass refinement to the cluster 'D' from DM S04. This cluster is well relaxed and isolated at  $z=0$  and has an average density profile and inner slope close to the mean value. First we mark all particles within one percent of the virial radius in the final halo and trace them back to the initial conditions. Then we add all particles within one comoving Mpc of a marked particle to the set of marked particles, and finally we add all particles which lie on intersections of any two already marked particles on the unperturbed initial grid positions. After these two steps there is a region with a fairly regular triaxial boundary which contains only marked particles. The number of marked particles grows by almost a factor of 8 during these additions, but it is still more than a factor of two smaller than the number of particles in the final cluster and a factor of ten smaller than the original high resolution volume used in DM S04. The computational cost with our code and parameters is roughly proportional to the number of high resolution particles, therefore we gain about a factor of ten with this reduction of the high resolution region. Probably one can reduce the high resolution volume further and focus even more of the computational effort into the innermost region, we plan to explore this possibility with future simulations.

## 2.2 Code and parameters

The simulations have been performed using PKDGRAV, written by Joachim Stadel and Thomas Quinn (Stadel 2001) using the same cosmological and numerical parameters as in DM S04 with a few changes given below and in Table 1. The cosmological parameters are ( $\Omega_m$ ;  $\Omega_b$ ;  $\sigma_8$ ;  $h$ ) =

(0.268; 0.732; 0.7; 0.71). The value of  $\sigma_8 = 0.9$  given in DM S04 is not correct: During the completion of this paper we found that due to a mistake in the normalization our initial conditions have less power than intended. This lowers the typical formation redshifts and halo concentrations slightly but does not affect the slopes of the inner density profiles.

We use the GRAFIC S2 package (Bertschinger 2001) to generate the initial conditions. The particle time-step criterion  $t_i < \frac{p_i}{m_i} = a_i$ , where  $a_i$  is the acceleration of particle ' $i$ ', gives almost constant time-steps in the inner regions of a halo (see Figure 2 in DM S04), but the dynamical times decrease all the way down to the center. Therefore the time-step criterion was slightly modified, to make sure enough time-steps are taken also near the halo centers: Instead of

$$t_i < \frac{p_i}{m_i} = a_i \quad (1)$$

we now use

$$t < \min\left(\frac{p_i}{m_i} = a_i, \frac{p_i}{G_i} = 4 \frac{G}{G_{\text{r}_i}}\right), \quad (2)$$

where  $\rho_i$  is the density at the position of particle ' $i$ ', obtained by smoothing over 64 nearest neighbors. We used  $\rho_i = 0.25$  for runs DM 25 and DM 50. Note that in the inner region of a CDM halo  $\rho(r) \propto r^{-3}$  ( $r < r_{\text{c}}$ ), i.e.  $0.8 \rho(r_{\text{c}}) = 0.25$  for  $r < r_{\text{c}}$  therefore the condition (2) with  $\rho_i = 0.25$  assures that at least 12 time-steps per local dynamical time  $\tau = \frac{p_i}{G_i} = 4 \frac{G}{G_{\text{r}_i}}$  are taken.

The time-steps are obtained by dividing the main time-step ( $t_0=200$ ) by a factor of two until condition (2) is fulfilled. In runs DM 25 and DM 50 the smallest particle time-steps are  $t_0=51200$ . According to Figure 2 in DM S04 this time-step is sufficient to resolve smaller scales than 0.1 percent of the virial radius, i.e. less than the limit set by the mass resolution, even in run DM 50.

The smaller time-steps in the inner regions of the cluster are crucial: In Figure 1 we compare two runs which only differ in the time-step criterion. DM 25lt was run with

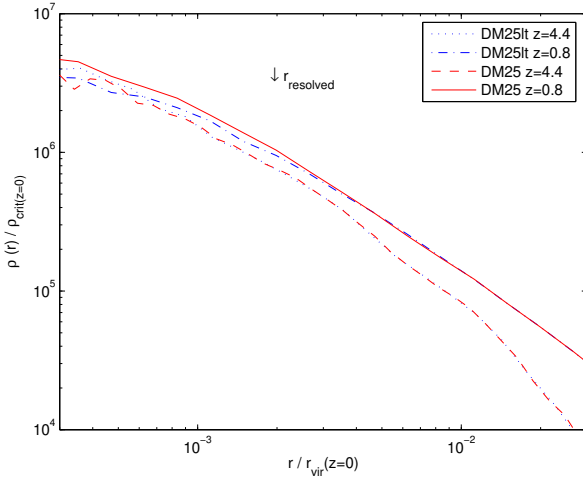


Figure 1. Density profiles in physical (not comoving) coordinates at redshifts 4.4 and 0.8. The two runs have equal mass resolution but different time-steps and softening. The arrow indicates the resolution limit set by the particle mass. The run with the larger time-steps and softening underestimates the dark matter density outside of the resolution scale.

the standard criterion (1) and  $\epsilon = 0.2$ , for run DM 25 we used the more stringent, computationally more expensive criterion (2) and  $\epsilon = 0.25$ . The difference in CPU time is about a factor of two. At  $z=0.8$  the densities in run DM 25lt are clearly lower out to 0.003 virial radii which also affects part of the region we aim to resolve with this run ( $r_{resolved} = 0.0019r_{vir}$ ). Due to the high computational cost of these runs we cannot perform a complete series of convergence test at this high resolution but due to the monotonic convergence behavior of PKDGRAV for shorter time-steps (Power et al. 2003) we are confident that DM 25 is a better approximation to the true CDM density profile of this cluster.

Our time-stepping test confirms that the time resolution in DM S04 was sufficient to resolve the minimum scale of 0.3% virial radii set by their mass resolution. For the purpose of this work, i.e. to resolve a region even closer to the center smaller time-steps are necessary. These two runs illustrate nicely how a numerical parameter or criterion that passes convergence tests performed at low or medium resolution can introduce substantial errors if employed in high resolution runs.

### 2.3 Testing the multimass technique

Reducing the high resolution region in the way described in Section 2.1 produces multimass virialised systems, i.e. halos where particles of different mass are mixed up with each other. The inner regions are dominated by light particles and the region near the virial radius by heavier particles. But one will find particles of both species everywhere in the final halo and one has to worry if this mixing introduces numerical effects, like energy transfer from the outer part to the inner part (from the heavy to the light particles)

due to two body interactions. This could lead to numerical softening of the density profile and make heavy particles sink to the center (Binney & Knebe 2002; Diem and et al. 2004a).

To check if the multimass technique works for cosmological simulations we re-ran the simulations D 6 and D 9 from DM S04 using a reduced high resolution region. We call these multimass runs 'DM 6se', 'DM 6le' and 'DM 9' (see Table 1). The next heavier particles in the surrounding region are 216 times more massive in DM 6se and DM 6le and 27 times more massive in DM 9. The heavier particles in DM 6le and DM 9 have larger softening to suppress discreteness effects while DM 6se uses the same small softening for both species. Figure 3 shows that the density profiles of the fully refined run D 9 and the partially refined run DM 9 are identical over the entire resolved range. Figure 2 shows that the same is true for run DM 6le, the larger mass ratio of 216 does not introduce any deviation from the density profile of the fully refined run.

A small softening in the heavier species (run DM 6sl) does introduce errors in the total density profile (Figure 2). The total mass profile is shallower near the resolved radius and has a high density bump below the resolved scale. The light particles are more extended and the bump is caused by a cold, dense condensation of six heavy particles within 0.004  $r_{vir}$ . These six heavy particles have a 3D velocity dispersion of only 273 km/s, while the light particles in the same region are much hotter,  $v_{3D} = 926$  km/s. They are hotter than the particles in the same region in run D 6 and DM 6le (both have only light particles in this inner part), the dispersion are 722 km/s for D 6 and 708 km/s for DM 6le.

These tests indicate that the reduced refinement regions work well in runs D 9M and DM 6le and therefore we used the same refinement regions to set up the higher resolution run DM 25. In this run the heavier particles are 125 times more massive than the high resolution particles and they have a softening of 9 kpc. For run DM 50 we refined only the inner part of the most massive cluster progenitor at  $z=4.4$  in the same way as the final cluster in runs DM 6le, DM 6se, DM 9 and DM 25. In run DM 50 the heavier particles are also 125 times more massive than the high resolution particles.

Figure 3 shows how the initially separated species of light and heavy particles mix up during the runs DM 9, DM 25 and DM 50. The density profiles of DM 6le and DM 9 do not suffer from numerical effects due to the multimass setup. This indicates that the same is true for run DM 25 which has the same refinement regions. In run DM 50 the amount and location of mixing at  $z=4.4$  relative to  $r_{200}$  is very similar to the situation if DM 9 at  $z=0.0$ , therefore we expect DM 50 to have the same density profile as a fully refined cluster, i.e. as a cluster resolved with a billion particles.

### 3 THE INNER DENSITY PROFILES

Here we try to answer the question if the inner density profiles of dark matter halos have a constant density or a cusp  $(r) \propto r^{-\gamma}$ . At resolutions of up to 25 million particles within the virial radius there is no evident convergence toward any constant inner slope (Fukushige et al. 2004; DM S04).

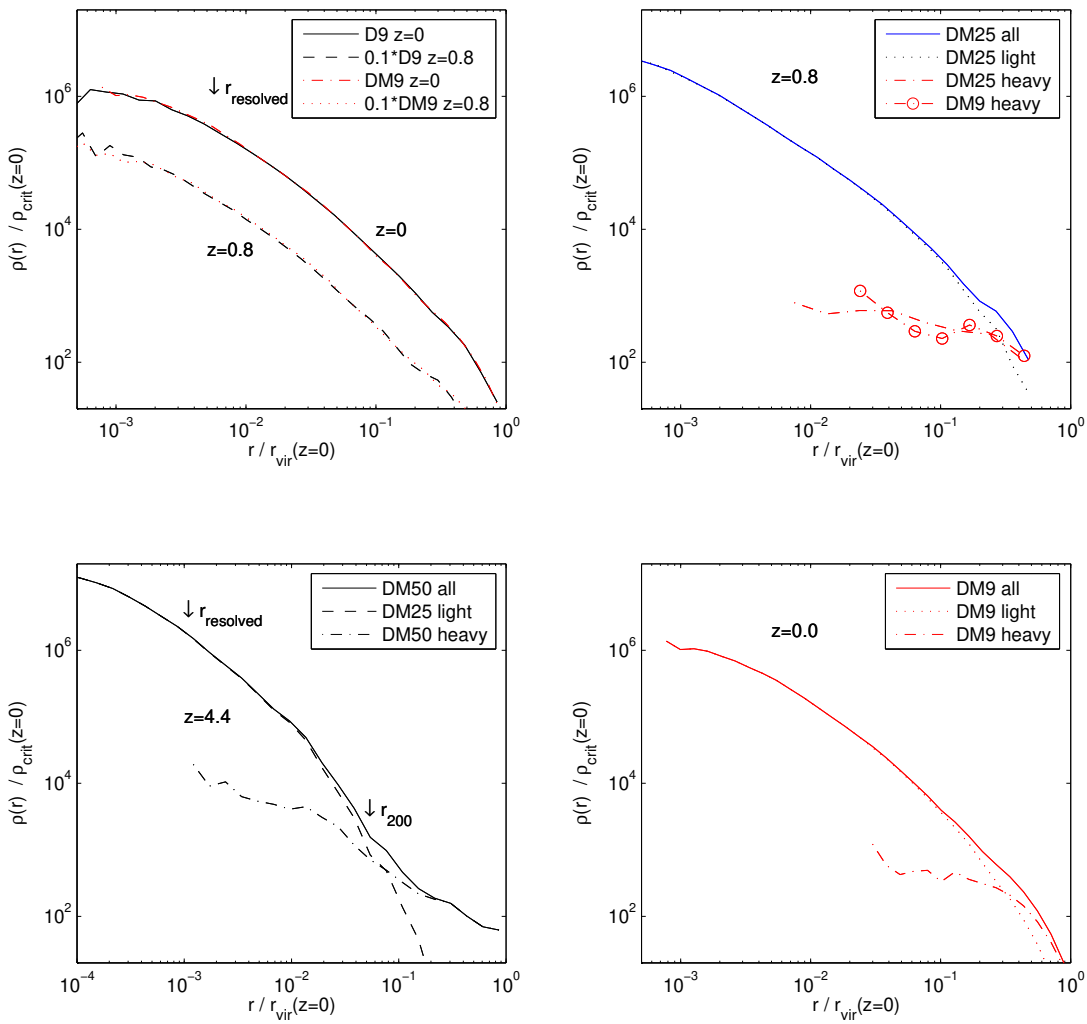


Figure 3. Tests of `multimass` refinement and convergence. The upper left panel shows that run D9 which contains only high resolution particles within the virial radius has the same density profile as the `multimass` run DM9. The  $z=0.8$  profiles are shifted downward by a factor of ten for clarity. The arrows indicate the convergence radius of run D9 estimated in DM S04. The lower left panel shows the high and low resolution particles in run DM50 at  $z=4.4$ . The panels on the right illustrate the mixing of light and heavy particles in runs DM9 and DM25 which have the same refinement regions.

### 3.1 Results of run DM 25

Run DM 25 has an effective resolution corresponding to 127 million particles within the virial radius and a force resolution of  $0.48 \times 10^{-3} r_{\text{vir}}$ . At this up to now unmatched resolution the inner slope is roughly constant from the resolved radius (see Figure 4) out to about one percent of the virial radius of the final cluster.

Run D 12 resolves the same cluster with 14 million particles and shows no convergence to a constant inner slope. Note that the 'D' cluster is one of six clusters analyzed in DM S04 and its inner profile is not special and rather close to the sample average.

Figure 4 indicates that there is a cusp in the centers of cold dark matter clusters and it becomes apparent only at this very high numerical resolution. The non-constant slopes just near the convergence scale are probably due to the first signs of numerical tattering that set in at this scale. At higher densities below the resolved scales one cannot make

any robust predictions yet, but if one has to extrapolate into this region Figure 4 motivates the choice of a cusp  $(r)/r \approx 12$ .

### 3.2 DM 50: estimating the profile of a billion particle halo

Mass accretion histories show that the inner part of CDM halos is assembled in an early phase of fast accretion (van den Bosch 2002; Wechsler et al. 2002; Zhao et al. 2003) and recent high resolution simulations revealed that the inner density profile does not evolve at low redshift (Fukushige, Kawai & Makino 2004; Tasitsiomi et al. 2004; Reed et al. 2005). Figure 4 confirms that the inner density profile of runs D 12 and D 5 do not change from  $z=0.8$  to  $z=0$ .

Therefore in run DM 50 we focus our computational effort even more on the early evolution of the inner profile. We refine the inner region of the most massive progenitor

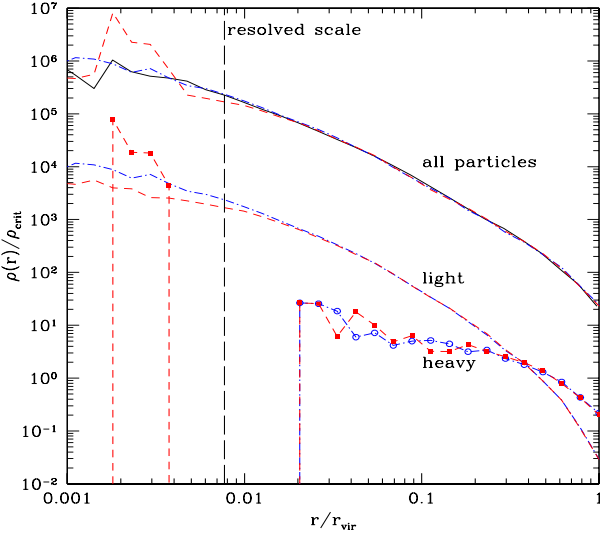


Figure 2. Tests of the multi-mass refinement technique. The upper three lines show the total density profile at  $z=0$  from the fully refined run D 6 (solid lines) and the multi-mass runs D M 6se (dashed) and D M 6le (dashed dotted). The lower lines (same line styles, offset by two magnitudes for clarity) show the density profiles of the two particle species, i.e. of the light ones (lines without symbols) and of the heavier ones (lines with symbols: filled squares for D 6se, open circles for D 6le). The vertical dashed line indicates the innermost resolved scale. In the multi-mass run with more softened heavier particles (D 6lh) the inner profile is dominated by light particles and identical to the fully refined run of the same cluster (D 6). When the heavier particles have short softenings some of them spiral into the center due to dynamical friction and transfer heat to the light particles. This affects the total density profile, i.e. it is lower near the resolved scale and has a bump due to a condensation of cold, massive particles very close to the center.

identified in run D M 25 at  $z=4.4$ . Since the refinement region needed is much smaller than the one of D M 9 or D M 25 and we only run the simulation to  $z=4.4$  it is feasible to go to a much better mass and force resolution. The high resolution particles in run D M 50 are a billion times lighter than the final cluster.

Figure 5 shows that the density profile of run D M 50 at  $z=4.4$  is cuspy down to the resolved radius ( $0.1\%$  of the virial radius). As in run D M 25 the slopes begin to shallow just at the converged scale due to numerical attenuation. The profile of D M 50 at  $z=4.4$  confirms the finding from run D M 25 that the inner profile follows a steep power law  $\propto r^{-1.2}$ , and at the higher resolution of D M 50 this is more evident.

Now we go one step further and use the information from all the 'D' -series runs to estimate the density profile one would obtain if one simulates this cluster with a billion particle all the way to present time, a run which would be possible but extremely expensive with today's computational resources. From Figure 6 one finds that the density profile of run D M 25 near its resolution scale shifts upward by a constant factor of 1.4 from  $z=4.4$  to  $z=0.8$ . The density around  $0.01 r_{\text{vir},z=0}$  is constant from  $z=0.8$  to  $z=0$ , see run D 5 in Figure 6. The inner density profile slopes are constant even longer, i.e. from  $z=4.4$  to  $z=0$ , see Figures 4 and

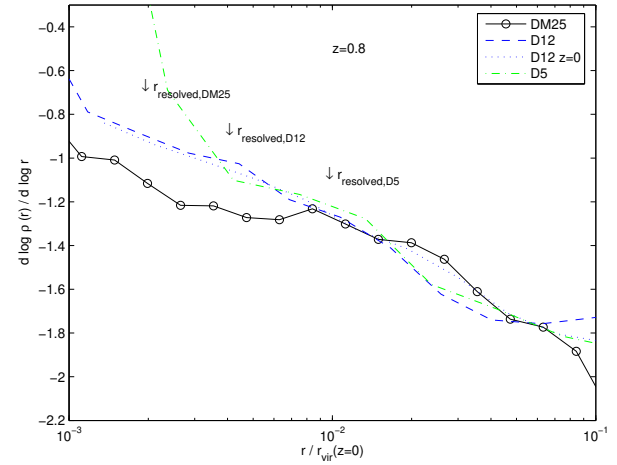


Figure 4. Logarithmic slope of the density profile of run D M 25 at  $z=0.8$ . The slopes of runs D 5 and D 12 at  $z=0.8$  and  $z=0$  are also shown for comparison. The arrows indicate the estimated convergence radii. Note that although the densities at the converged scales are within 10 percent the density gradients can already be substantially smaller.

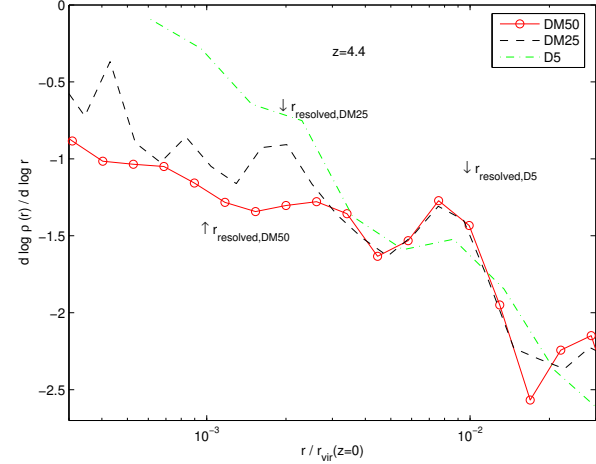


Figure 5. Logarithmic slope of the density profile of run D 5, D M 25 and D M 50 at  $z=4.4$ . The arrows indicate the estimated convergence radii. A constant inner slope of about -1.2 is evident in the highest resolution run D M 50. The increase of the slopes around the resolved radii is due to the onset of numerical attenuation.

5. Therefore we estimate the  $z=0$  profile of run D M 50 by rescaling the  $z=4.4$  profile of D M 50 by a factor 1.4 and using the  $z=0$  profile of run D 12 outside of  $0.005 r_{\text{vir},z=0}$  (see Figure 6).

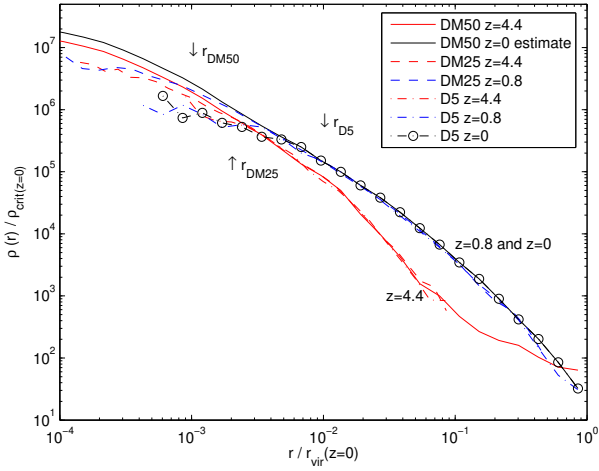


Figure 6. Density profiles in physical (not comoving) coordinates at redshifts 4.4, 0.8 and 0. A arrow s mark the resolved scales of each run. The densities in the inner part do not evolve between  $z=0.8$  and  $z=0$  and the inner slopes remain constant even from  $z=4.4$  to  $z=0$ . Using these observations we are able to estimate the profile of a billion particle halo (upper solid line).

### 3.3 Cored and cuspy fitting functions

In this section we fit one cuspy and two recently proposed cored functions to the density profiles of DM 25 at  $z=0.8$  and to the estimated profile of DM 50 at  $z=0.0$ . From the last section we expect the cuspy function to work better in the inner part but we try to fit also the cored profiles for comparison.

We use a general profile that asymptotes to a central cusp ( $r$ ) /  $r$  :

$$g(r) = \frac{s}{(r=r_s) (1 + (r=r_s))^{1-\gamma}} : \quad (3)$$

If one takes  $s$ ,  $\gamma$  and  $r_s$  as free parameter one encounters strong degeneracies, i.e. very different combinations of parameter values can fit a typical density profile equally well (Klypin et al. 2001). Therefore we fix the outer slope  $\gamma = 3$  and the turnover parameter  $s = 1$ . For comparison the NFW profile has  $(\gamma, s) = (1, 3; 1)$ , the M 99 profile has  $(\gamma, s) = (15, 3; 15)$ . We fit the three parameters  $\gamma$ ,  $r_s$  and  $s$  to the data.

Navarro et al. (2004) proposed a different fitting function which curves smoothly over to a constant density at small radii:

$$\ln(g_N(r)) = s_N (2 = N) [(r=r_s)^N - 1] \quad (4)$$

$N$  determines how fast this profile turns away from a power law in the inner part. Navarro et al. (2004) found that  $N$  is independent of halo mass and  $N = 0.172 \pm 0.032$  for all their simulations, including galaxy and dwarf halos.

Another profile that also curves away from power law behavior in the inner part was proposed by Stoehr et al. (2002):

$$_{\text{SWTS}}(r) = \frac{V_{\text{max}}^2}{4G} 10^{-2 \alpha_{\text{SWTS}} \log \frac{r}{r_{\text{max}}}} \frac{1}{r^2}$$

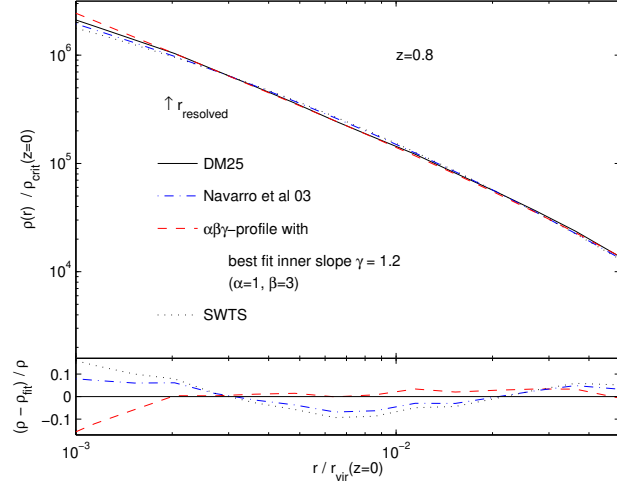


Figure 7. Density profile of run DM 25 at  $z=0.8$  and fits with three different functions.

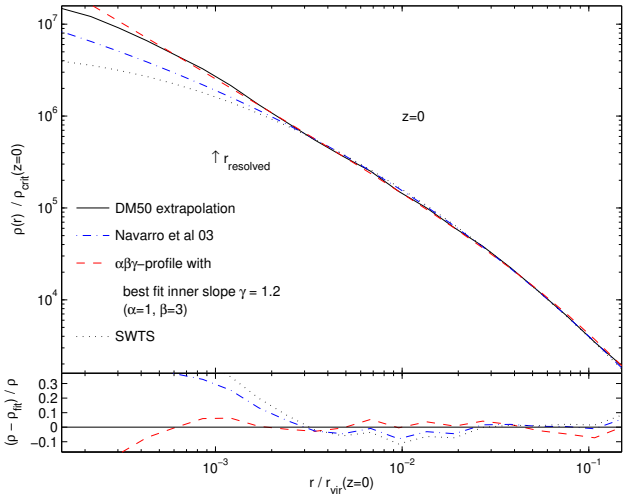


Figure 8. Density profile of run DM 50 extrapolated to  $z=0.0$  and fits with three different functions.

$$h = 1 - 4 \alpha \log \frac{r}{r_{\text{max}}} \quad (5)$$

where  $V_{\text{max}}$  is the peak value of the circular velocity,  $r_{\text{max}}$  is the radius of the peak and  $\alpha_{\text{SWTS}}$  determines how fast the profile turns away from a power law near the center. Stoehr (2004) found that cluster profiles are well fitted with this formula using  $\alpha_{\text{SWTS}}$  values between 0.093 and 0.15.

These three functions were fitted to the data from  $z=0.8$  by minimizing the relative density differences in each of about 20 logarithmically spaced bins in the range resolved by DM 25 (i.e. from  $0.0019r_{\text{vir};z=0} = 3.3$  kpc to  $r_{\text{vir};z=0} = 1750$  kpc). At  $z=0$  we use the resolved range of D 12 for the fits (i.e. from  $0.0039r_{\text{vir};z=0} = 6.8$  kpc to  $r_{\text{vir};z=0}$ ). The resulting best fit values and the root mean squares of the relative density differences are given in Table 2.

Table 2. Density profile parameters of run DM 25 at  $z=0.8$  and of DM 50 extrapolated to  $z=0$ .  $\sigma$  is the root mean square of  $(\rho - \bar{\rho})^2$  for the three fitting functions used.

redshift	G	$r_{\text{SG}}$ [kpc]	G	N	$r_{\text{SN}}$ [kpc]	N	$\sigma_{\text{SW TS}}$	$r_{\text{max SW TS}}$ [kpc]	SW TS
0.8	1.20	260	0.075	0.157	233	0.076	0.130	565	0.087
0.0	1.20	283	0.059	0.162	236	0.133	0.140	518	0.179

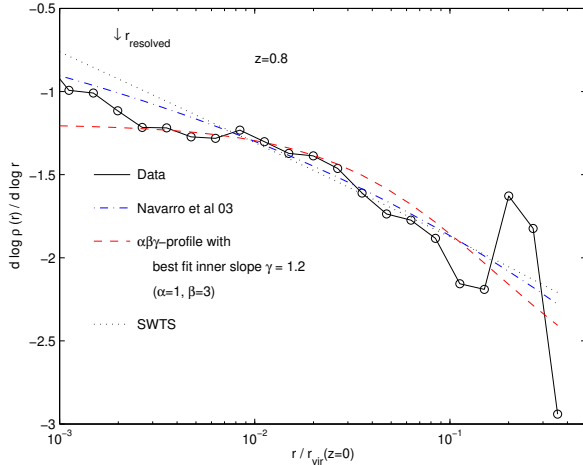


Figure 9. Logarithmic slopes of the measured and fitted density profiles from Figure 7.

At  $z=0.8$  the average residuals of the three fits are similar, but they are dominated by the contribution from the outer parts of the cluster (see Figure 6 in DM 04). Figures 7 and 8 show that in the inner part the cuspy profile describes the data better. Both cored profiles underestimate the measured density at the resolution limit both at  $z=0.8$  and  $z=0$ . These profiles lie below the measured density profiles even inside of  $r_{\text{resolved}}$  where one has to expect that the next generation of simulations will be able to resolve even higher densities.

Figures 9 and 10 show the slopes of the simulated profile in comparison with the slopes of the best fits. Again it is evident that in the inner part the cuspy profile describes the real density run much better.

#### 4 CONCLUSIONS

The main conclusions of this work are the following:

It is possible to use different mass particles to resolve one halo in cosmological CDM simulations without affecting the resulting density profiles.

This "multimass" technique allows a reduction of the necessary number of particles and the computational cost by at least one order of magnitude without loss of resolution in the central region of the halo.

We confirm that the inner profile of a typical CDM cluster does not evolve since about redshift one.

The logarithmic slope of the dark matter density profile converges to a roughly constant value in the inner part

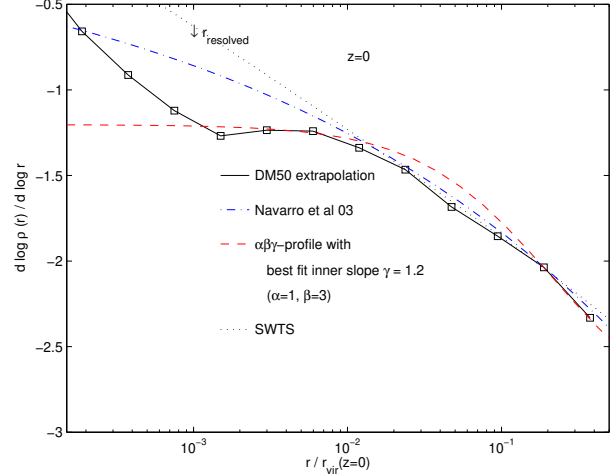


Figure 10. Logarithmic slopes of the measured and fitted density profiles from Figure 8.

of cluster halos. This probably holds also for smaller systems (like galaxy and dwarf halos) but there it is even more difficult to numerically resolve the cusps.

At resolutions around 10 million particles per halo the inner slope appears to approach zero continuously but this impression is caused by numerical softening of the profiles due to insufficient mass resolution.

The cluster studied here has a central cusp  $\rho \propto r^{-\gamma}$  with a slope of about  $\gamma = 1.2$ . From earlier studies (DM 04) we expect this inner profile to be close to the average and the scatter is about 0.15.

Profiles with a core (Stoehr et al. 2002; Navarro et al. 2004) underestimate the measured dark matter density at (and even inside of) the current resolution limit.

#### ACKNOWLEDGMENTS

We like to thank Piero Madau and Mike Kuhlen for useful discussions and the referee for valuable suggestions. All computations were performed on the zBox supercomputer at the University of Zurich. J.D. is supported by the Swiss National Science Foundation.

#### REFERENCES

Ahn K. J., Shapiro P. R., preprint, arXiv:astro-ph/0412169.  
 Bertone G., Merritt D., 2005, Mod. Phys. Lett. A, 20, 1021

Bertschinger E., 2001, *ApJSS*, 137, 1

Binney J., 2004, *MNRAS*, 350, 939

Binney J., Knebe A., 2002, *MNRAS*, 333, 378

Calzaneo-Roldan C., Moore B., 2000, *PhRvD*, 62, 123005

Colin P., Avila-Reese V., Valenzuela O., 2000, *ApJ*, 542, 622

Colin P., Klypin A., Valenzuela O., & Gottlöber, S., 2004, *ApJ*, 612, 50

Dawson J.M., 1983, *Rev. Mod. Phys.*, 55, 403

DeBlok W.J., McGaugh S.S., Bosma A., Rubin V.C., 2001, *ApJ*, 552, L23

Diemand J., Moore B., Stadel J., Kazantzidis S., 2004a, *MNRAS*, 348, 977

Diemand J., Moore B., Stadel J., (‘DM S04’), 2004b, *MNRAS*, 353, 624

Diemand J., Moore B., Stadel J., 2005, *Nature*, 433, 389

Flores R.A., Primack J.R., 1994, *ApJ*, 427, L1

Fukushige T., Makino J., 1997, *ApJ*, 477, L9

Fukushige T., Makino J., 2003, *ApJ*, 588, 674

Fukushige T., Kawata A. and Makino J., 2004, *ApJ*, 606, 625

Gao L., White S.D.M., Jenkins A., Frenk C., Springel V., preprint, arXiv:astro-ph/0503003.

Ghigna S., Moore B., Governato F., Lake G., Quinn T., Stadel J., 1998, *MNRAS*, 300, 146

Ghigna S., Moore B., Governato F., Lake G., Quinn T., Stadel J., 2000, *ApJ*, 544, 616

Hansen S.H., Moore B., arXiv:astro-ph/0411473.

Klypin A., Kravtsov A.V., Bullock J.S., Primack J.R., 2001, *ApJ*, 554, 903

Kuhlen M., Strigari L.E., Zentner A.R., Bullock J.S., Primack J.R., 2005, *MNRAS*, 357, 387

Macchio A.V., Quercellini C., Mainini R., Amendola L., Bonometto S.A., 2004, *Phys. Rev. D*, 69, 123516

Moore B., 1994, *Nature*, 370, 629

Moore B., Diemand J., Stadel J., 2004, *IAU Colloq. 195: Outskirts of Galaxy Clusters: Intense Life in the Suburbs*, 513

Moore B., Governato F., Quinn T., Stadel J., Lake G., 1998, *ApJ*, 499, L5

Moore B., Quinn T., Governato F., Stadel J., Lake G., 1999, *MNRAS*, 310, 1147

Moore B., Calzaneo-Roldan, C., Stadel, J., Quinn, T., Lake, G., Ghigna, S., Governato, F., 2001, *Phys. Rev. D* 64, 063508

Navarro J.F., Frenk C.S., White S.D.M., 1996, *ApJ*, 462, 563

Navarro J.F., Hayashi E., Power C., Jenkins A., Frenk C.S., White S.D.M., Springel V., Stadel J., Quinn T.R., 2004, *MNRAS*, 349, 1039

Power C. et al., 2003, *MNRAS*, 338, 14

Piada F., Klypin A., Flix J., Martinez M., Simonneau E., 2004, preprint, arXiv:astro-ph/0401512.

Reed D., Governato F., Verde L., Gardner J., Quinn T., Stadel J., Merritt D., Lake G., 2005, *MNRAS*, 357, 82

Salucci, P., Burkert, A., 2000, *ApJ*, 537, L9

Simon J.D., Bolatto A.D., Leroy A., Blitz L., Gates E.L., 2005, *ApJ*, 621, 757

Springel V., White S.D.M., Tormen G., Kauffmann G., 2001b, *MNRAS*, 328, 726

Stadel J., 2001, PhD thesis, U. Washington

Stoehr F., 2004, preprint, arXiv:astro-ph/0403077.

Stoehr F., White S.D.M., Tormen G., Springel V., 2002, *MNRAS*, 335, L84

Swaters R.A., Moore B.F., van den Bosch F.C., Baloëls M., 2003, *ApJ*, 583, 732

Tasitsiomi I.A., Kravtsov A.V., Gottlöber S., Klypin A.A., 2004, *ApJ*, 607, 125

van den Bosch F.C., Swaters R.A., 2001, *MNRAS*, 325, 1017

van den Bosch F.C., 2002, *MNRAS*, 331, 98

Wechsler R.H., Bullock J.S., Primack J.R., Kravtsov A.V., Dekel A., 2002, *ApJ*, 568, 52

Zhao D., Mo H., Jing Y., G. Boerner G., 2003, *MNRAS*, 339, 12

This paper has been typeset from a *TeX* / *ETEX* file prepared by the author.